Brazilian Journal of Biology®

ISSN 1519-6984 (Print)
ISSN 1678-4375 (Online)

Original Article

Morphometry, topography and arterial supply of the thyroid gland in rhesus monkeys (*Macaca mulatta* Zimmermann, 1780)

Morfometria, topografia e suprimento arterial da glândula tireoide em macacos rhesus (*Macaca mulatta* Zimmermann, 1780)

A. V. Stocco[a], R. Medeiros-do-Nascimento[a], C. T. Messias[b], C. A Santos-Sousa[c*], P. Souza-Junior[d], A. Pissinatti[e] and M. Abidu-Figueiredo[a]

[a] Universidade Federal Rural do Rio de Janeiro – UFRRJ, Departamento de Anatomia Animal e Humana, Seropédica, RJ, Brasil
[b] Universidade Federal do Acre – UFAC, Centro de Ciências Biológicas e da Natureza, Rio Branco, AC, Brasil
[c] Universidade Federal dos Vales do Jequitinhonha e Mucuri – UFVJM, Instituto de Ciências Agrárias, Unaí, MG, Brasil
[d] Universidade Federal do Pampa – UNIPAMPA, Departamento de Medicina Veterinária, Uruguaiana, RS, Brasil
[e] Centro de Primatologia do Rio de Janeiro – CPRJ, Instituto Estadual do Ambiente, Guapimirim, RJ, Brasil

Abstract

The purpose of this research was to investigate the measures, topography, and vascularization of the thyroid gland in *Macaca mulatta*, a non-human primate. The study involved the dissection of ten male adult cadavers of *Macaca mulatta*. The length, width, and thickness of the right lobe of the thyroid were 2.552 ± 0.341, 1.019 ± 0.137, and 0.729 ± 0.137 cm. These measures in the left thyroid lobe were 2.406 ± 0.299, 1.013. ± 0.087, and 0.769 ± 0.083 cm. The study found no significant differences in the measures of the left and right lobes of the thyroid gland in rhesus monkeys. Regarding topography, the thyroid gland was located ventrolateral to the trachea, similar to its position in other mammal species. The cranial pole of the gland was closely related to the cricoid or thyroid cartilage, while the caudal pole showed variable positioning to the tracheal rings. The isthmus, a thin band of tissue connecting the lobes, was present in all specimens. The cranial thyroid artery was found to originate from the external carotid artery in most specimens. It supplied the thyroid gland and sent branches to muscles in the neck region. The caudal thyroid artery, originating from the common carotid artery, provides additional blood supply to the gland and sends a branch to the esophagus. This research contributes to knowledge about the thyroid gland in non-human primates, specifically *Macaca mulatta*. The findings provide critical information for comparative studies and understanding the thyroid gland's role in health and disease.

Keywords: animal anatomy, endocrine organ, experimental model, primates.

Resumo

O objetivo desta pesquisa foi investigar as medidas, topografia e vascularização da glândula tireoide em *Macaca mulatta*, uma espécie de primata não humano. O estudo envolveu a dissecação de dez cadáveres adultos machos de *Macaca mulatta*. O comprimento, largura e espessura do lobo direito da tireoide foram de 2,552 ± 0,341, 1,019 ± 0,137 e 0,729 ± 0,137 cm, respectivamente. Essas medidas no lobo esquerdo da tireoide foram de 2,406 ± 0,299, 1,013 ± 0,087 e 0,769 ± 0,083 cm, respectivamente. O estudo não encontrou diferenças significativas nas medidas dos lobos esquerdo e direito da glândula tireoide em macacos rhesus. Quanto à topografia, a glândula tireoide estava localizada ventrolateralmente à traqueia, similar à sua posição em outras espécies de mamíferos. O polo cranial da glândula estava intimamente relacionado à cartilagem cricoide ou tireoide, enquanto o polo caudal mostrava posicionamento variável em relação aos anéis traqueais. O istmo, uma fina faixa de tecido que conecta os lobos, estava presente em todos os espécimes. A artéria tireoide cranial foi encontrada originando-se da artéria carótida externa na maioria dos espécimes. Ela supria a glândula tireoide e enviava ramos para músculos na região do pescoço. A artéria tireoide caudal, originária da artéria carótida comum, fornecia suprimento adicional de sangue à glândula e enviava um ramo ao esôfago. Esta pesquisa contribui para o conhecimento sobre a glândula tireoide em primatas não humanos, especificamente em *Macaca mulatta*. Os achados fornecem informações críticas para estudos comparativos e para entender o papel da glândula tireoide na saúde e na doença.

Palavras-chave: anatomia animal, órgão endócrino, modelo experimental, primatas.

*e-mail: carlos-augusto.ca@ufvjm.edu.br
Received: October 7, 2023 – Accepted: December 20, 2023

1. Introduction

Throughout history, animals have been used for scientific studies, including research on anatomy, physiology, pathology, and pharmacology (Andersen and Winter, 2019). Non-human primates, in particular, have been extensively used in animal research due to their genetic, behavioral, and biochemical similarities to humans. Rhesus monkeys (*Macaca mulatta*), for instance, are commonly used as non-human primate models for studying and validating various clinical and surgical procedures, particularly in assessing thyroid function (Ozpinar et al., 2010, 2011).

The thyroid gland is an essential endocrine organ that regulates numerous physiological processes such as metabolism, growth, development (Nussey and Whitehead, 2001) and behavioral (Foda and Shams, 2021). Investigating the anatomy of the thyroid gland in primates can provide valuable insights into the evolution and function of this vital organ in humans and other primates (Casteleyn and Bakker, 2022). Comparative studies of the thyroid gland in primates can also help researchers understand how differences in thyroid gland anatomy and function have evolved in response to different environmental and ecological pressures. For example, humans' relatively large thyroid gland compared to other primates has been suggested to reflect a greater demand for more sustained exertion in humans compared to a more intermittent activity in non-humans (Crile, 1934).

Moreover, studying the thyroid gland in primates can help researchers comprehend the organ's role in various disease states, including thyroid disorders such as hyperthyroidism and hypothyroidism. By comparing the thyroid gland anatomy and function in healthy and diseased primates, researchers can gain insights into the underlying mechanisms of these disorders and develop more effective treatments (Casteleyn and Bakker, 2022).

In humans, the thyroid gland is located in the midline of the lower neck, consisting of the right and left lobes typically connected by an isthmus in the midline. It lies anterolateral to the larynx and trachea at approximately the level of the second and third tracheal rings and weighs about 30 grams (Policeni et al., 2012; Akudu et al., 2018). The thyroid gland is attached to the larynx and trachea within the visceral space, surrounded by the infrahyoid strap muscles (sternohyoid and sternothyroid), and moves with the larynx during swallowing (Policeni et al., 2012; Akudu et al., 2018). The thyroid gland receives its blood supply from the superior and inferior thyroid arteries, which have several anastomoses providing a rich vascular supply to the gland (Dessie, 2018).

The purpose of this research was to characterize the measures, topography, and vascularization of the thyroid gland in *Macaca mulatta*, a non-human primate species commonly used in scientific research.

2. Materials and Methods

This study is part of a larger project called "Basic and Applied Research in the Morphology of Rhesus Monkeys (*Macaca mulatta*)." The project was approved by the Ethics Committee of the Universidade Federal Rural do Rio de Janeiro (CEUA Protocol No. 014/2015). Ten male adult cadavers of *Macaca mulatta* were donated to the Departamento de Anatomia Animal e Humana da Universidade Federal Rural do Rio de Janeiro by the Centro de Criação de Animais de Laboratório (CeCAL) from Fundação Oswaldo Cruz (Fiocruz).

For this study, the common carotid artery was accessed via a medial ventral cervical incision, dissected in situ, and cannulated to wash the vascular system with saline solution and fixed it with 10% formaldehyde. Next, a colored-stained Petrolax S-65 was used to fill the vascular system. The cadavers were then immersed in a low-density polyethylene container with a capacity of 500 liters, containing a 30% formaldehyde solution to finalize the fixation and latex polymerization process.

After this period, dissections were performed on the skin and the ventral muscles of the neck to expose the trachea, thyroid glands, and arteries. The thyroid glands were dissected in situ to characterize their topography, and digital calipers were used to measure their length, width, and thickness. The origin of the thyroid arteries was also determined. The dissected samples were imaged using a Nikon Coolpix® L820 model camera. The study adopted the official veterinary anatomical nomenclature (ICVGAN, 2017).

The mean and standard deviation of the thyroid measurements were calculated and compared in both antimeres using an unpaired t-test. A p-value less than 0.05 was considered statistically significant.

3. Results

The average thyroid lobe length, width, and thickness measured 2.48 ± 0.32, 1.02 ± 0.11, and 0.75 ± 0.11 cm, respectively. These measurements did not differ between antimers ($p > 0.05$) (Table 1 and Figure 1). In this sample, the thyroid lobe gland length varied from 2.11 to 3.14 cm, the width from 0.74 cm to 1.26 cm, and the thickness from 0.54 to 0.98 cm. A thin isthmus was present in all the analyzed specimens and measured 0.79 ± 0.25 cm in width. Most of the lobes were positioned cranially at the level of the cricoid cartilage and caudally at the seventh tracheal ring (Table 2 and Figure 2). The lobes were situated over the cricoid cartilage to the fifth tracheal ring. Nevertheless, many lobes extended as rostral as the level of the thyroid cartilage's caudal horn, and some as caudal as the eighth tracheal ring level.

The external carotid artery gave rise to the cranial thyroid artery in all the samples (Figure 3), except in

Table 1. Average ± standard deviation (cm) of thyroid gland lobes measures in male rhesus monkeys (*Macaca mulatta*) (n = 10).

	Right lobe	Left lobe	p-value
Length	2.55 ± 0.341	2.40 ± 0.30	0.32
Width	1.02 ± 0.137	1.01 ± 0.09	0.91
Thickness	0.73 ± 0.137	0.77 ± 0.08	0.44

one animal where the cranial thyroid artery originated at the internal carotid artery bilaterally. Besides the thyroid gland, the cranial thyroid artery sent branches to the sternothyroid, cricothyroid, and thyrohyoid muscles (Figure 4). The caudal thyroid artery originated from the common carotid artery and gave a branch to the esophagus (Figure 5). However, one specimen had no branch to the sternothyroid muscle bilaterally.

Table 2. Absolute and percentage frequencies of the right and left thyroid lobes, cranial and caudal limits to the level of the cricoid or thyroid cartilages and tracheal rings in male rhesus monkeys (*Macaca mulatta*) (n = 10).

	Right	Left
CHTC to 5th TR	2 (20%)	1 (10%)
CHTC to 6th TR	1 (10%)	2 (20%)
CHTC to 7th TR	1 (10%)	2 (20%)
CHTC to 8th TR	1 (10%)	-
CC to 6th TR	1 (10%)	2 (20%)
CC to 7th TR	4 (40%)	3 (30%)

CHTC: caudal horn of thyroid cartilage; **CC**: cricoid cartilage; **TR**: tracheal ring.

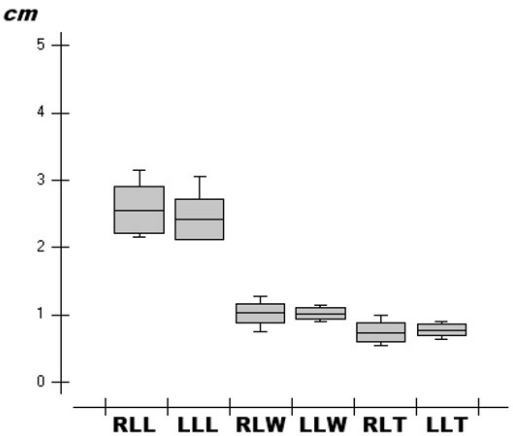

Figure 1. Box-plot graph representing the comparison of the measures of the right lobe length (**RLL**), the left lobe length (**LLL**), the right lobe width (**RLW**), the left lobe width (**LLW**), the right lobe thickness (**RLT**), and the left lobe thickness (**LLT**).

4. Discussion

4.1. Measures

Limited data regarding the morphometry, topography, and vascularization of the thyroid gland in primates are available. This study found no differences between the left and right lobes of the thyroid gland in rhesus monkeys, consistent with previous studies on other mammal species such as Santa Inês sheep (Lima et al., 2009), domestic dogs (Rodrigues et al., 2016), and Brazilian Shorthair Cats (Stocco et al., 2021). However, Novo et al. (2009) reported larger measurements for the left lobe than the right lobe in dogs using ultrasonographic examination. Santos et al. (2008) observed differences in width measurements between the left and right lobes in European taurine fetuses, with higher values for the left lobe. In addition, Joshi et al. (2010) studied human male cadavers and found asymmetry between the right and left lobes of the thyroid gland, with slightly different measurements for height and thickness.

A limitation of this present study is that the differences in thyroid measurements between sexes could not be evaluated because the sample was composed of male rhesus monkeys. However, Santos et al. (2008) reported differences between males and females only for the length of the left lobe in bovine fetuses. Silva et al. (2019) found asymmetries in the mean thickness of the right lobe between males and females and the length of the left lobe between the sexes in rabbits.

4.2. Topography

The thyroid gland in rhesus monkeys was located ventrolateral to the trachea, similar to many other domestic and wild mammals (Akudu et al., 2018; Borges et al., 2019; Carvalho et al., 2003; König and Liebich, 2016; Policeni et al., 2012; Rodrigues et al., 2016; Silva et al., 2019; Stocco et al., 2021; Yamasaki, 1990, 1996, 2016). However, koalas arranged it laterally to the trachea at the clavicle level (Yamasaki, 1993). In addition, the cranial pole of the gland in rhesus monkeys had a close relationship with the cricoid or thyroid cartilage. In contrast, the caudal pole showed a variable topographic relation to the tracheal rings.

In this study's specimens, the thyroid gland consisted of two lobes joined by an isthmus. An isthmus is typical in higher primate species, including humans, according to Vázquez et al. (2006). However, Crile (1937) reported no thyroid isthmus in three specimens of rhesus monkeys.

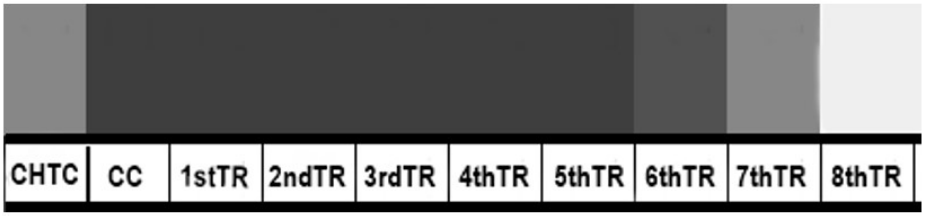

Figure 2. Graphic illustration of the anatomical positioning of the thyroid gland lobes to the larynx and trachea. Darker areas represent positions where the lobes were most frequently distributed. **CHTC**: caudal horn of thyroid cartilage; **CC**: cricoid cartilage; **TR**: tracheal ring.

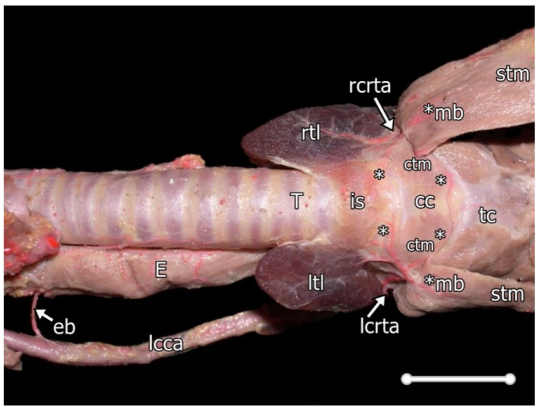

Figure 3. Photomacrography of the ventral view of the thyroid gland of a rhesus monkey showing its morphology, topography and vascularization. **T** – trachea, **E** – esophagus, **tc**- thyroid cartilage, **cc** – cricoid cartilage, **ctm** – cricothyroid muscle, **stm** - sternothyroid muscle, ***mb** – muscular branches, **muscular banches for isthmus and cricothyroid muscle, **is** – isthmus, **rcrta** – right cranial thyroid artery, **rtl** – right thyroid lobe, **lcrta –** left cranial thyroid artery, **ltl** – left thyroid lobe, **lcca** – left common carotid artery, **eb –** esophageal branch. Scale bar: 2cm.

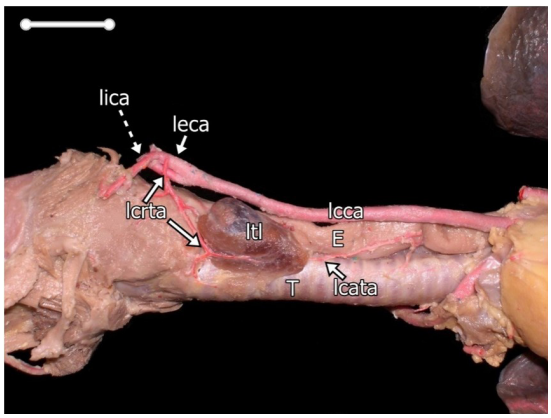

Figure 4. Photomacrography of the left lateral view of the thyroid gland of a rhesus monkey showing its topography and vascularization. **T** – trachea, **E** – esophagus, **lica** – left internal carotid artery, **leca** – left external carotid artery, **lcrta** – left cranial thyroid artery, **lcata** – left caudal thyroid artery, **ltl** – left thyroid lobe, **lcca** - left common carotid artery. Scale bar: 2cm.

The isthmus we visualized were fragile and pale and perhaps become unnoticed in the previous study. Joshi et al. (2010) observed that the isthmus was absent in 16% cases out of the human male cadavers they studied. Ranade et al. (2008) described the absence of an isthmus in 33 percent of the human specimens they examined.

In *Cavia cobaya* (Yamasaki, 1994), the thyroid lobes, located laterally to the trachea, showed a uniform morphology, with an isthmus occurring in only a few males and females out of the 60 specimens studied. In New Zealand rabbits, the isthmus was present in all the analyzed animals, connecting the left and right lobes of the thyroid gland

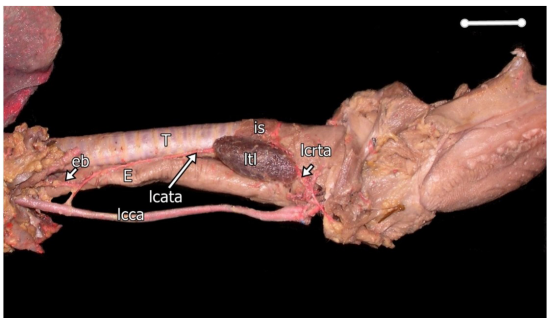

Figure 5. Photomacrography of the left lateral view of the thyroid gland of a rhesus monkey showing its topography and vascularization. **T** – trachea, **E** – esophagus, **lcrta** – left cranial thyroid artery, **ltl** – left thyroid lobe, **is** – isthmus, **lcca** - left common carotid artery, **eb** – esophageal branch, **lcata**- left caudal thyroid artery. Scale bar: 2cm.

(Borges et al., 2019). The topography of the thyroid lobes in New Zealand rabbits varied, with the cranial extremity typically at the level of the cricoid cartilage and the caudal end showing more variability, ranging from the third to the tenth tracheal ring (Silva et al., 2019). In Brazilian Shorthair Cats (Stocco et al., 2021), most lobes had their cranial pole at the level of the first tracheal ring and the caudal lobe at the eighth tracheal ring. However, some lobes had their cranial pole located as cranially as the level of the cricoid cartilage and the caudal pole as caudally as the 12th tracheal ring. Most samples showed symmetrical cranial pole locations for both the left and right lobes at the same tracheal ring level, with the isthmus being apparent in a higher percentage of male cats than female cats.

4.3. Vascularization

The vascularization of the thyroid gland in rhesus monkeys was investigated in this study. The cranial (superior) thyroid artery was found to originate from the external carotid artery in 90% of the specimens, consistent with previous reports (Castelli and Huelke, 1965). However, an exception was observed in one animal where the cranial thyroid artery originated from the internal carotid artery bilaterally. The cranial thyroid artery also supplied the thyroid gland and sent branches to the sternothyroid, cricothyroid, and thyrohyoid muscles.

Similar to findings in dogs (Rodrigues et al., 2016), wild cats (Carvalho et al., 2003), and ruminants (Santos et al., 2008; Lima et al., 2009), both the cranial (superior) and caudal (inferior) thyroid arteries provided blood supply to both lobes of the thyroid gland in all dissected monkeys. Furthermore, these arteries originated from the external carotid artery, which is consistent with observations made by Dessie (2018) in human cadavers.

In our study, the cranial thyroid artery exhibited variations in branching patterns, supplying the sternohyoid muscle, sternothyroid muscle, cricothyroid muscle, thyrohyoid muscle, and esophagus, similar to observations in human cadavers (Dessie, 2018).

According to Castelli and Huelke (1965) and Policeni et al. (2012), in humans, the inferior thyroid artery arises from

the thyrocervical trunk, a branch of the subclavian artery. It courses anterior to the vertebral artery and longus colli muscle. The superior thyroid artery, on the other hand, is the first branch of the external carotid artery, originating just below the hyoid bone. However, Dessie (2018) observed variations in the origin of the superior thyroid artery, with it arising from the external carotid artery in 44.2% of cases, common carotid bifurcation in 27.9% of cases, and common carotid artery in 26.7% of cases.

In humans, the superior thyroid artery originated from the external carotid artery in 97% of cases on the right side and 95.5% on the left side, with variations in origin observed in a small percentage of cases. The inferior thyroid artery often originated from the thyrocervical trunk, with some variations noted (Özgüner and Sulak, 2014).

Yamasaki (1990) conducted a study on rats and found that the cranial and caudal thyroid arteries were present in the vascularization of the thyroid gland, originating from the external carotid artery in most cases. Furthermore, Yamasaki (1995) observed significant variations in the number of thyroid arteries in Guinea pigs, with up to five types of artery arrangements observed. However, in our study, the cranial (superior) and caudal (inferior) thyroid arteries were found to supply blood to both lobes of the thyroid gland.

Understanding rhesus monkeys' topography and vascularization of the thyroid gland provides valuable insights for clinical approaches and surgical procedures. Moreover, knowledge of potential anatomical variations in the thyroid gland is crucial for procedures such as thyroid resection, tumor removal, and tracheostomy.

Acknowledgements

This study was financed in part by National Council of Technological and Scientific Development (CNPq), Rio de Janeiro State Research Foundation (FAPERJ) and Coordination of Superior Level Staff Improvement (CAPES) Finance Code 001.

References

AKUDU, L.S., UKOHA, U.U., EKEZIE, J. and UKOHA, C.C., 2018. Ultrasonographic study of the incidence of pyramidal lobe and agenesis of the thyroid isthmus in Nnewi population. *Journal of Ultrasonography*, vol. 18, no. 75, pp. 290-295. http://dx.doi.org/10.15557/JoU.2018.0042. PMid:30763012.

ANDERSEN, M.L. and WINTER, L.M.F., 2019. Animal models in biological and biomedical research: experimental and ethical concerns. *Anais da Academia Brasileira de Ciências*, vol. 91, suppl. 1, e20170238. http://dx.doi.org/10.1590/0001-3765201720170238. PMid:28876358.

BORGES, A.P.S., MENEZES, L.T., SANTOS, L.A., HERRERA, G.C., FRANÇA, G.L., DE PAULA, S.Y.A., HIRAKI, K.R.N. and SILVA, F.O.C., 2019. Topography, irrigation, and histology of the thyroid gland of New Zealand rabbits (*Oryctolagus cuniculus* Linnaeus, 1758). *International Journal of Advanced Engineering Research and Science*, vol. 6, no. 3, pp. 225-229. http://dx.doi.org/10.22161/ijaers.6.3.29.

CARVALHO, S.F.M., SANTOS, A.L.Q., ANDRADE, M.B., MAGALHAES, L.M., RIBEIRO, F.M., CRUZ, G.C. and MALTA, T.S., 2003. Morfometria e vascularização arterial da glândula tireóide do gato mourisco, Herpailurus yagouaroundi (Severtzow, 1858) felidae. *Ars Veterinária*, vol. 19, no. 3, pp. 216-218.

CASTELEYN, C. and BAKKER, J., 2022. *Anatomy of the Rhesus Monkey (Macaca mulatta): the essentials for the biomedical researcher*. London: IntechOpen, 326 p.

CASTELLI, W.A. and HUELKE, D.F., 1965. The arterial system of the head and neck of the rhesus monkey with emphasis on the external carotid system. *The American Journal of Anatomy*, vol. 116, no. 1, pp. 149-169. http://dx.doi.org/10.1002/aja.1001160108. PMid:14283279.

CRILE, G., 1934. *Diseases peculiar to civilized man*. New York: MacMillan.

CRILE, R., 1937. The comparative anatomy of the thyroid and adrenal glands in wild animals. *The Ohio Journal of Science*, vol. 37, no. 1, pp. 42-61.

DESSIE, M.A., 2018. Variations of the origin of superior thyroid artery and its relationship with the external branch of superior laryngeal nerve. *PLoS One*, vol. 13, no. 5, e0197075. http://dx.doi.org/10.1371/journal.pone.0197075. PMid:29746515.

FODA, D.S. and SHAMS, S.G., 2021. A trial for improving thyroid gland dysfunction in rats by using a marine organism extract. *Brazilian Journal of Biology = Revista Brasileira de Biologia*, vol. 81, no. 3, pp. 592-600. http://dx.doi.org/10.1590/1519-6984.226829. PMid:32935817.

INTERNATIONAL COMMITTEE ON VETERINARY GROSS ANATOMICAL NOMENCLATURE – ICVGAN, 2017. *Nomina Anatomica Veterinaria.* 6th ed. Hannover: Editorial Committee, 178 p.

JOSHI, S.D., JOSHI, S.S., DAIMI, S.R. and ATHAVALE, S.A., 2010. The thyroid gland and its variations: a cadaveric study. *Folia Morphologica*, vol. 69, no. 1, pp. 47-50. PMid:20235050.

KÖNIG, H.E. and LIEBICH, H.G., 2016. *Anatomia dos animais domésticos: texto e atlas colorido*. 6ª ed. Porto Alegre: Artmed.

LIMA, E.M.M., FERREIRA, P.M., SILVA, L.R.E., VIANNA, A.R.C.B., SANTANA, M.I.S., SILVA, F.O.C.E. and SEVERINO, R.S., 2009. Morfometria e suprimento arterial da glândula tireoide em ovinos da raça Santa Inês. *Veterinaria Noticias*, vol. 15, no. 1, pp. 35-40.

NOVO, A.C.M.P., CARVALHO, C.B. and ALVES, R.B.M., 2009. Ultrassonografia das glândulas tireóideas em cães (*Canis familiaris*, Linnaeus, 1758). *Journal of Brazilian Animal Science*, vol. 2, no. 3, pp. 135-149.

NUSSEY, S. and WHITEHEAD, S., 2001. *Endocrinology: an integrated approach*. Oxford: BIOS Scientific Publishers.

ÖZGÜNER, G. and SULAK, O., 2014. Arterial supply to the thyroid gland and the relationship between the recurrent laryngeal nerve and the inferior thyroid artery in human fetal cadavers. *Clinical Anatomy*, vol. 27, no. 8, pp. 1185-1192. http://dx.doi.org/10.1002/ca.22448. PMid:25130905.

OZPINAR, A., BRUSS, M., SHELTON, D. and GILLESPIE, J., 2010. Thyroidal radioactive iodide uptake in the lactating rhesus monkey. *Laboratory Animals*, vol. 44, no. 2, pp. 155-158. http://dx.doi.org/10.1258/la.2009.009014. PMid:19959568.

OZPINAR, A., GOLUB, M.S., POPPENGA, R.H., BLOUNT, B.C. and GILLESPIE, J.R., 2011. Thyroid status of female rhesus monkeys and preliminary information on impact of perchlorate administration. *Laboratory Animals*, vol. 45, no. 3, pp. 209-214. http://dx.doi.org/10.1258/la.2011.010047. PMid:21669905.

POLICENI, B.A., SMOKER, W.R. and REEDE, D.L., 2012. Anatomy and embryology of the thyroid and parathyroid glands. *Seminars*

in Ultrasound, CT, and MRI, vol. 33, no. 2, pp. 104-114. http://dx.doi.org/10.1053/j.sult.2011.12.005. PMid:22410358.

RANADE, A.V., RAI, R., PAI, M.M., NAYAK, S.R., PRAKASH., KRISNAMURTHY, A. and NARAYANA, S., 2008. Anatomical variations of the thyroid gland: possible surgical implications. *Singapore Medical Journal*, vol. 49, no. 10, pp. 831-834. PMid:18946620.

RODRIGUES, A.B.F., COSTA, N.Q., AGUIAR, R.R., DI FILIPPO, P.A. and ALMEIDA, A.J., 2016. Análise morfológica, topográfica e vascularização da glândula tireóide em cães (*Canis familiaris*). *Revista Brasileira de Medicina Veterinária*, vol. 38, no. 3, pp. 316-322.

SANTOS, A.L.Q., MAXIMIANO NETO, A., MOURA, L.R., PEREIRA, H.C. and SILVA JÚNIOR, L.M.D.A., 2008. Vascularização arterial, forma, topografia e morfometria da glândula tireóide em fetos de bovinos com sangue europeu. *Veterinaria Noticias*, vol. 14, no. 1, pp. 63-70.

SILVA, S.C., STOCCO, A.V., SANTOS-SOUSA, C.A., ESTRUC, T.M., MARQUES, L.E., SOUZA-JUNIOR, P. and ABIDU-FIGUEIREDO, M., 2019. Morfometría y vascularización de la glándula tiroides en conejo (*Oryctolagus cuniculus*). *International Journal of Morphology*, vol. 37, no. 4, pp. 1404-1408. http://dx.doi.org/10.4067/S0717-95022019000401404.

STOCCO, A.V., PEÇANHA, S.V., NASCIMENTO, R.M., SANTOS-SOUSA, C.A., SOUZA JÚNIOR, P. and FIGUEIREDO, M.A., 2021. Morphometry, topography and arterial supply of the thyroid gland in Brazilian shorthair cats. *Acta Scientiae Veterinariae*, vol. 49, pp. 1-8. http://dx.doi.org/10.22456/1679-9216.114452.

VÁZQUEZ, J.P., VERONA, J.G., PAZ FERNÁNDEZ, F.J. and CACHORRO, M.B., 2006. Agenesis of the thyroid isthmus. *European Journal of Anatomy: Official Journal of the Spanish Society of Anatomy*, vol. 10, no. 2, pp. 83-84.

YAMASAKI, M., 1990. Comparative anatomical studies of thyroid and thymic arteries: I. Rat (*Rattus norvegicus albinus*). *The American Journal of Anatomy*, vol. 188, no. 3, pp. 249-259. http://dx.doi.org/10.1002/aja.1001880304. PMid:2371965.

YAMASAKI, M., 1993. Comparative anatomical studies on the thyroid and thymic arteries. II. Polyprotodont marsupials. *Journal of Anatomy*, vol. 183, no. Pt 2, pp. 359-366. PMid:8300422.

YAMASAKI, M., 1995. Comparative anatomical studies on the thyroid and thymic arteries. III. Guinea pig (*Cavia cobaya*). *Journal of Anatomy*, vol. 186, no. 2, pp. 383-393. PMid:7649838.

YAMASAKI, M., 1996. Comparative anatomical studies on the thyroid and thymic arteries. IV. Rabbit (*Oryctolagus cuniculus*). *Journal of Anatomy*, vol. 188, no. Pt 3, pp. 557-564. PMid:8763473.

YAMASAKI, M., 2016. Comparative anatomical studies on the thyroid and thymic arteries. VI. Diprotodont marsupials. *Anatomical Science International*, vol. 91, no. 3, pp. 258-273. http://dx.doi.org/10.1007/s12565-015-0293-y. PMid:26472114.